INSTITUTE OF PHYSICS PUBLISHING NANOTECHNOLOGY
Nanotechnology **14** (2003) 1239–1245 PII: S0957-4484(03)66806-6

Ultrasensitive label-free DNA analysis using an electronic chip based on carbon nanotube nanoelectrode arrays

Jessica Koehne, Hua Chen[1], Jun Li[2], Alan M Cassell[1], Qi Ye[1], Hou Tee Ng[1], Jie Han[1] and M Meyyappan

NASA Ames Research Center, Moffett Field, CA 94035, USA

E-mail: jli@mail.arc.nasa.gov

Received 31 July 2003, in final form 26 September 2003
Published 17 October 2003
Online at stacks.iop.org/Nano/14/1239

Abstract
We report the detection of DNA PCR amplicons using an ultrasensitive label-free electronic technique based on multiwalled carbon nanotube (MWNT) nanoelectrode arrays embedded in an SiO_2 matrix. Specific PCR amplicons are reliably detected using electrochemical (EC) methods through allele-specific oligonucleotide hybridization. The inherent guanine bases in the DNA amplicon target of ∼300 bases serve as signal moieties with the aid of $Ru(bpy)_3^{2+}$ mediators, providing an amplified anodic current associated with the oxidation of guanine groups at the nanoelectrode surface. The reduced size and density of the nanoelectrode array provided by MWNTs dramatically improves the sensitivity of EC detection. In addition, the abundant guanine bases in target DNA produce a large signal. Less than ∼1000 target amplicons can be detected on a microspot, approaching the sensitivity limit of conventional laser-based fluorescence techniques. This method also eliminates the labelling requirement and makes the measurements much simpler. This platform can be employed for developing highly automated electronic chips with multiplex nanoelectrode arrays for quick DNA analysis.

1. Introduction

Electrochemical (EC) methods are attractive for providing simple and low-cost solutions to DNA analysis [1–5]. Individually addressed microelectrode arrays have been demonstrated in DNA analysis based on allele-specific oligonucleotide (ASO) hybridization, which can be directly integrated with microelectronics and microfluidics systems to gain advantages in miniaturization, multiplexing and automation [2–5]. However, the sensitivity of DNA detection using EC methods [3–5] is normally significantly lower than conventional laser-based fluorescence techniques. In a previous report [6], we demonstrated that nanostructured elements such as multiwalled carbon nanotube (MWNT) could be employed as a nanoelectrode array to improve the detection sensitivity. The hybridization of less than 10^6 oligonucleotide targets [6] can be measured using a MWNT nanoelectrode array on a $20 \times 20\ \mu m^2$ contact pad combined with $Ru(bpy)_3^{2+}$ mediated guanine oxidization [7]. Here we further demonstrate that unlabelled PCR amplicon can be directly measured with EC techniques using MWNT nanoelectrode arrays. Since a large number of inherent guanine bases in the long single-stranded PCR amplicon serve as signal moieties, the detection limit can be further lowered by orders of magnitude to under ∼1000 target DNAs, approaching the sensitivity limit of conventional fluorescence based DNA microarray techniques [8]. Consistent results are demonstrated in measuring a specific PCR amplicon in comparison with those in four types of control experiments. The label-free nature, ultrahigh sensitivity, high reliability and simple operation of this electronic method has great potential in developing low-cost disposable chips for quick DNA analysis.

[1] ELORET Corporation, Sunnyvale, CA 94087, USA.
[2] Author to whom any correspondence should be addressed.

Well-defined MWNT nanoelectrode arrays are fabricated on silicon chips using a bottom-up scheme [6, 9, 10]. The processing involves: (1) lithographic patterning, (2) metallization of electrical contacts, (3) catalyst deposition, (4) MWNT growth by plasma enhanced chemical vapour deposition (PECVD), (5) SiO_2 dielectric encapsulation, and (6) chemical mechanical polishing (CMP). In the previous report [6], we demonstrated that the location and density of MWNTs could be precisely controlled by advanced lithographic techniques based on e-beam, focused ion beam, EUV or nanoimprinting. However, these techniques are expensive and not readily available. Here we demonstrate a much simpler processing solution, requiring only a minimum effort with conventional photolithography, to obtain low-density MWNT nanoelectrode arrays, which is critical in achieving the ultrahigh sensitivity. This solution makes it possible to mass fabricate the MWNT nanoelectrode array chip at minimum cost.

2. Experimental methods

2.1. Electrode preparation

MWNT growth by PECVD and SiO_2 gapfilling by tetraethoxysilane (TEOS) CVD follow the conditions reported before [6, 9, 10]. The typical sample size is $\sim 1 \times 1$ cm^2. CMP is carried out with a vibratory polisher (Vibromet 2, Buehler, IL, USA). The progress of the polishing process is monitored by measuring electrical resistance between two points at the polished surface and further confirmed with scanning electron microscopy (SEM) (S4000, Hitachi, Japan) and occasionally with transmission electron microscopy (TEM) (2000FX, JEOL, Japan). The MWNT nanoelectrode is electrochemically etched at 1.50 V (versus SCE) in 1.0 M NaOH for 30–150 s to improve the EC activity and provide well-defined functional groups at the MWNT ends. The nanoelectrode behaviour is confirmed with the cyclic voltammetry (CV) measurements of 5.0 mM $K_4[Fe(CN)_6]$ in 1.0 M KCl, typically showing a sigmoidal shape in the CV curve. Over-polished samples give high-density MWNT nanoelectrode arrays typically showing CV curves similar to that obtained with a macroelectrode due to the heavy overlap of diffusion layers from individual nanoelectrodes. Such samples are not suitable for high sensitivity DNA detection and thus rejected.

2.2. Probe immobilization

A 10 μM oligonucleotide probe of [Cy3]5′-CTIIATTT-CICAIITCCT-3′ [AmC7-Q] (QIAGEN, CA, USA) in a 50 μl PBS buffer is mixed with coupling reagents of 0.5 mg 1-ethyl-3(3-dimethyl aminopropyl) carbodiimide hydrochloride (Fluka, Switzerland) and 0.25 mg *N*-hydroxysulfo-succinimide (Aldrich, WI, USA). The reaction mixture is applied to the freshly EC-etched CNT nanoelectrode array, and incubated at room temperature for about 1 h. The primary amine groups in the oligonucleotide probes form amide bonds with the –COOH groups at the CNT ends. Nonspecific binding is eliminated by stringent washes in three steps using 2 × SSC/0.1% SDS, 1 × SSC, and 0.1 × SSC, respectively, by shaking the sample in each solution at 40 °C for 15 min. The fluorescence image of the Cy3 tag in the immobilized probe is taken with a laser scanner (GMS417, Genetic Micro Systems, MA, USA) to confirm immobilization. Furthermore, the probe densities from the fluorescence measurements are correlated with EC measurements.

2.3. PCR amplification and hybridization

Genomic DNA from a healthy donor is used in PCR to amplify

(1) a normal allele of ∼300 bases within a BRCA1 gene containing 5′-AGGACCTGCGAAATCCAG-3′ which is complementary to the specific oligo-probe, and
(2) an unrelated normal allele of ∼400 bases within a BRCA1 gene, with a thermocycler (PTC-200, MJ Research, MD, USA) [11].

The presence of the PCR amplicons are confirmed with gel electrophoresis versus a DNA molecular weight standard (ΦX174RFDNA-HaeIII digest, Invitrogen, CA, USA). The PCR products are purified and desalted on QIAquick spin columns with ddH_2O used as the eluent. The double stranded PCR targets are denatured at 95 °C for 5 min and quenched in an ice bath prior to hybridization, which is carried out by incubating the probe-functionalized electrodes in ∼0.1 μM target solutions in a 3 × SSC buffer over 2 h at 40 °C. A solution containing 10 μM of 20 mer polyG in PBS is also used as the target solution in control experiments at the same incubation conditions. The electrodes are then washed with 2 × SSC/0.1% SDS, 1 × SSC, and 0.1 × SSC at 40 °C for 15 min, respectively.

2.4. Electrochemical detection

All EC experiments are carried out with an Autolab potentiostat (GSTAT12, Ecochemie, The Netherlands) in a three-electrode setup using a Pt coil counter electrode and a SCE reference electrode. The size of the working electrode is defined with a 3 mm i.d. O-ring sealed in a Teflon cell. AC voltammetry (ACV) is measured in 5.0 mM $Ru(bpy)_3^{2+}$ with 0.20 M NaOAc (pH = 5.2) using an AC sinusoidal wave at 10 Hz and 25 mV amplitude superimposed on the staircase DC potential ramp from 0.50 to 1.20 V. Differential pulse voltammetry (DPV) using pulses with 25 mV amplitude is also employed in a few experiments, which gives similar results as ACV with slightly smaller peak widths and larger peak heights.

3. Results

The principles of nanoelectrode array based DNA sensors are illustrated in figure 1 while the detailed structure and fabrication processes are described later. Forest-like vertical MWNT arrays are directly grown by PECVD on individually addressed metal microcontacts as shown in figure 1(a). Each microcontact can be varied from 20 to 400 μm in size using normal photolithography. MWNT arrays and the substrate surface are encapsulated in SiO_2 with only the ends of a small amount of MWNTs exposed at the surface and used as inlaid nanodisk electrode arrays. The MWNTs at each microcontact spot are functionalized with a specific oligonucleotide probe so that multiplex detection can be achieved. Typically,

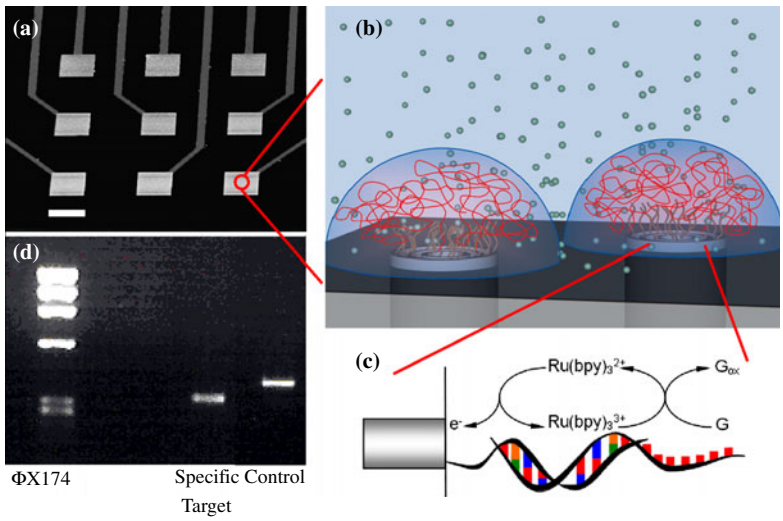

Figure 1. (a) An SEM image of an individually addressable 3 × 3 microcontact array with a MWNT nanoelectrode array on each site. The scale bar is 200 μm. (b) Schematic of the mechanism to detect DNA hybridization using a MWNT nanoelectrode array. The long single-stranded DNA PCR amplicons are hybridized to the short oligonucleotide probes which are functionalized at the very end of the MWNTs. $Ru(bpy)_3^{2+}$ mediators are used to transfer electrons from the guanine groups to the MWNT nanoelectrode for all target molecules within the hemispherical diffusion layer of the nanoelectrodes. (c) The schematic mechanism for the guanine oxidation amplified with $Ru(bpy)_3^{2+}$ mediators. (d) The gel electrophoresis. The lanes from left to right are DNA molecular weight standard (ΦX174RFDNA-HaeIII digest), a specific PCR amplicon target with ∼300 bases, and a control sample with an unrelated PCR amplicon with ∼400 bases, respectively.

about 100 MWNT nanoelectrodes or more are produced on each microcontact to form a local nanoelectrode array. For maximizing the sensitivity at each microsensing spot, the density of MWNT nanoelectrodes has to be controlled at a very low value (typically $<5 \times 10^7$ electrode cm^{-2}) so that the diffusion layers of neighbouring electrodes will not overlap. An array of ∼100 MWNT nanolectrodes at each microcontact is desired to provide good statistics and reliability without significantly sacrificing the sensitivity.

Figures 1(b) and (c) show the schematic mechanism of the MWNT nanoelectrode array for DNA detection. Since the EC etching produces abundant –COOH groups at the end of MWNTs similar to graphite edge-planes [12], primary amine terminated oligonucleotide probes can be selectively functionalized to MWNTs by forming amide bonds [6]. In the previous report, we estimated an upper limit of ∼9000 –COOH sites on each MWNT (∼100 nm in diameter) based on the CV data of surface bound ferrocene derivatives [6]. A specific probe [Cy3]5′ CTIIATTTCICAIITCCT-3′ [AmC7-Q] is used in this study, which contains the sequence of the normal allele of the BRCA1 gene associated with the occurrence of several cancers [13]. Electroactive guanine groups in the probe are replaced with nonelectroactive inosines to avoid unnecessary background noise from the probe molecules without affecting base-pairing. Due to the size of the probe molecules, it is likely that less than 10% of the –COOH functional sites are used, giving less than 900 probes on each MWNT.

Genomic DNA from a healthy donor is used in PCR to amplify:

(1) a normal allele of ∼300 bases within the BRCA1 gene containing 5′-AGGACCTGCGAAATCCAG-3′, which is complementary to the specific oligonucleotide probe, and
(2) an unrelated normal allele of ∼400 bases within the BRCA1 gene [11].

Figure 1(d) shows the electrophoresis results of a DNA molecular weight standard (ΦX174RFDNA-HaeIII digest) and the two PCR amplicons, respectively. Considering the physical size (radius of gyration of ∼6 nm for ssDNA with 300 bases [14]), it is expected that no more than ∼70 targets can be hybridized with the probes on each MWNT of ∼100 nm diameter. The nonspecific binding is removed by stringent washing in three steps using 2 × SSC/0.1% SDS, 1 × SSC, and 0.1% SSC respectively, by shaking the sample in the solution at 40 °C for 15 min. The nonhybridization portion of the target molecules likely dangles near to, but may not be necessarily in direct contact with, the electrode surface as shown in figure 1(b). $Ru(bpy)_3^{2+}$ mediators are used to efficiently transport electrons from the guanine bases to the MWNT nanoelectrodes and provide an amplified guanine oxidation signal [15] as long as target DNA molecules are within the three-dimensional diffusion layer (typically a hemisphere with a radius of ∼300 nm, i.e. $\sim 6R_{ave}$, where R_{ave} is the average nanoelectrode radius [16]).

For ease of experiment, the results reported here were obtained with MWNT nanoelectrode arrays on $\sim 1 \times 1$ cm^2 macroscopic metal contacts, confirmed with microsamples. Figure 2(a) shows a SEM image of an as-grown MWNT array on a catalyst film deposited on a Si substrate covered with 200 nm continuous Cr film. The forest-like MWNT array has a narrow size distribution and good vertical alignment. The diameter is uniform along the tube axis and can be varied from 20 to 200 nm by tuning PECVD conditions and the thickness of the catalyst film. The average tube–tube distance is ∼300 nm. These MWNTs are produced by a tip growth mechanism leaving Ni catalyst particles at the tip as shown by the TEM image in figure 2(b). For an array with ∼10 μm average height, the variation is within $\sim \pm 1.5$ μm. These MWNTs have a bamboo-like structure with a series of closed graphitic shells along the tube axis.

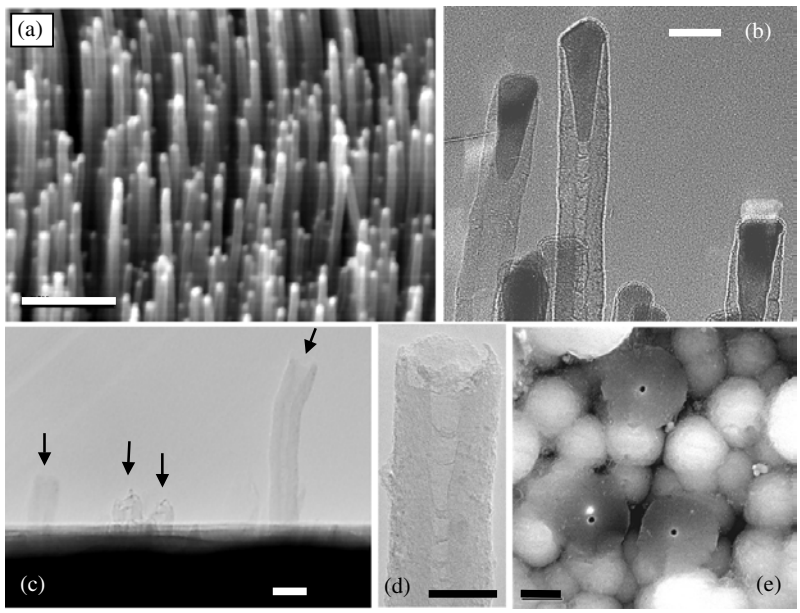

Figure 2. (a) An SEM image of the as-grown CNT array, (b) a high-resolution TEM image of the tip of the as-grown CNTs showing a bamboo-like multiwalled structure, (c) a cross-sectional TEM image of the MWNTs protruding over the SiO_2 matrix after CMP, (d) a high-resolution TEM image of the open end of a MWNT, and (e) an SEM image of an embedded low-density MWNT nanoelectrode array after EC etching. The scale bars are 1 μm, 50 nm, 50 nm, 20 nm, and 1 μm, respectively.

After encapsulation and proper CMP, a planarized SiO_2 surface is generated with only the end of some MWNTs exposed. Due to higher mechanical resilience, MWNTs get polished slower than SiO_2, leaving a portion of ∼10–100 nm protruding over the SiO_2 surface. Figure 2(c) shows the cross-sectional TEM image of a planarized MWNT array in a SiO_2 matrix. Clearly, the top part of the MWNTs is removed, resulting in open ends. The high-resolution TEM image in figure 2(d) shows that the MWNT maintains the highly ordered graphitic structure resulting in an ideal electrode similar to the graphite edge plane [12] which is known to have a fast electron transfer rate, wide potential window, flexible surface chemistry and good biocompatibility. The closed shells in the bamboo-like structure, despite not being ideal for fast electron transfer[3], is sufficient for the present purposes. The closed shells also keep the electrolytes from filling the entire hollow channel of MWNTs, thus reducing the background signal, which is desired for achieving ultrahigh sensitivity for electroanalysis. To further minimize the background current and produce a carboxylic acid terminated surface for probe functionalization, MWNTs are electrochemically etched until their ends are approximately level with the SiO_2 surface. Figure 2(e) shows the SEM image of an etched MWNT nanoelectrode array, where dark spots correspond to the very end of the MWNTs.

The performance of an electrode with respect to temporal and spatial resolution is known to scale inversely with the electrode radius [17–19]. Therefore, the sensitivity can be dramatically improved by reducing the size of the electrodes to the nanoscale. Indeed, using a Pt–Ir electrode with 15 nm diameter, Fan and Bard [19] were able to detect a single redox molecule. Nanoelectrode arrays fabricated in filtration membranes also demonstrated orders of magnitude lower detection limits compared to conventional macroelectrodes (1.6 nM versus 1.6 μM) [20]. In our study, the present fabrication method allows us to control the MWNT nanoelectrode array at sufficiently low density, with an average tube–tube spacing over 2.5 μm. As a result, the overlap of the diffusion layers from neighbouring nanoelectrodes is minimized and each one behaves as a single nanoelectrode.

In general, it is difficult to reproducibly fabricate nanoelectrode arrays with desired low-density without using advanced lithography based on e-beam, EUV and focused ion beam, which are expensive and not readily available. However, since MWNTs in the as-grown array have rather uniform diameter but varying heights (as shown in figure 2(b)), different densities can be easily obtained by stopping CMP at the proper stage. Figure 3(a) shows a SEM image of a MWNT array right after encapsulation in SiO_2. During CMP, more and more MWNTs are exposed as shown in figures 3(b)–(d), which can be easily monitored by measuring the electrical resistance (R) between two points at the surface. A calibration curve in figure 3(e) shows the value of R versus the time at the final stage of CMP. The resistance R drops exponentially with time and saturates at about 50–80 Ω, where almost all MWNTs are exposed. In this study, all samples have R over 400 Ω, corresponding to an average tube–tube distance over 2.5 μm, which are also confirmed with SEM.

Figure 4(a) shows three consecutive ACV scans of a probe-functionalized MWNT nanoelectrode array after hybridizing to the specific PCR amplicon with ∼300 bases. Well-defined peaks are observed around 1.04 V, with the first scan (red curve) clearly higher than the second (blue dotted curve) and the third (black curve) scans, while the latter two are nearly superimposed on each other. The baselines are flat and stable.

[3] The electrical resistance along a single MWNT grown by PECVD in our study is ∼5–10 times higher than a perfect MWNT grown by high temperature methods such as arc discharge and laser ablation [9] and [10]. As reported in [6], a well prepared high-density CNT array typically gives a peak separation of ∼100 mV in CV measurements in 1 mM $K_4[Fe(CN)_6]$ in 1.0 K KCl, bigger than the ∼60 mV value obtained with graphite edge-plane electrodes.

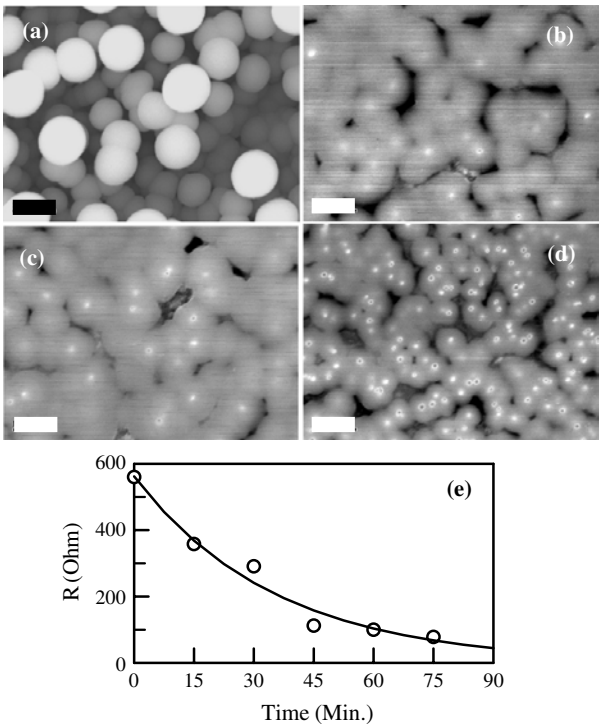

Figure 3. SEM images of (a) an as-encapsulated MWNT array in SiO_2, and (b)–(d) the polished surface showing that the number of exposed MWNTs increases during the CMP process. All scale bars are 1 μm. (e) The calibration curve used for controlling the density of exposed MWNTs. The electrical resistance decays exponentially versus the time near the final stage of CMP. SEM images in (b)–(d) correspond to the point at 0, 15 and 75 min, respectively.

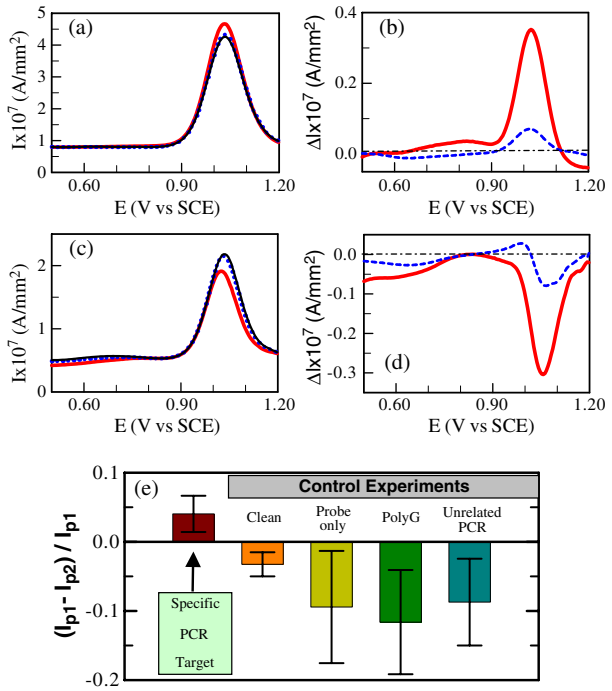

Figure 4. (a) Three consecutive ACV measurements (first—red curve, second—blue dotted curve, and third—black curve) and (b) the differential curves between the first and the second scans ($\Delta I_{1,2} = I_1 - I_2$)—red curve, and that between the second and the third scans ($\Delta I_{2,3} = I_2 - I_3$)—blue dashed curve, of a CNT nanoelectrode array functionalized with BRCA1 probes and hybridized with the specific PCR amplicon. (c) and (d) are similar measurements after incubating with the unrelated PCR amplicon. The black dash–dot curves in (b) and (d) represent the background current. The measurements were carried out in 5 mM $Ru(bpy)_3^{2+}$ and 0.20 M NaOAC (pH = 5.2) with an AC sinusoidal wave of 10 Hz and 25 mV amplitude on top of a staircase DC ramp. (e) Summary of the mean value and the standard deviation of $(I_{p1} - I_{p2})/I_{p1}$ from 21 measurements at five different conditions: (1) probe-functionalized MWNT nanoelectrode array incubated in specific PCR amplicon target, (2) unfunctionalized clean MWNT nanoelectrode array, (3) probe-functionalized MWNT nanoelectrode array alone, (4) probe-functionalized MWNT nanoelectrode array incubated in a 20 mer polyG solution, and (5) probe-functionalized MWNT nanoelectrode array incubated in unrelated PCR amplicon.

The anodic current peaked around 1.04 V consists of the contribution from two parts:

$$I = I_{\text{mediators}} + I_{\text{amplifiedG}} \tag{1}$$

where $I_{\text{mediators}}$ is from the oxidation of $Ru(bpy)_3^{2+}$ mediators in the bulk electrolyte solution, and $I_{\text{amplifiedG}}$ is the anodic current associated with the oxidation of guanine groups in the target DNA molecules which are attached to the surface through specific hybridization with the probe molecules. These two reactions happen to occur at almost the same potential, i.e. 1.04 V. $I_{\text{amplifiedG}}$ is approximately proportional to the number of guanine groups at the surface. In principle, one can directly measure the oxidation current from guanine groups alone (i.e. I_G) without adding $Ru(bpy)_3^{2+}$ mediators to the electrolyte solution. However, as we demonstrated in a previous report [6], the signal was very low due to the extremely small number of DNA molecules that we were detecting. To achieve ultrahigh sensitivity, the signal of guanine oxidation has to be amplified. $Ru(bpy)_3^{2+}$ mediator has been demonstrated to be very efficient in amplifying the guanine oxidation signal [5, 7]. This mechanism provides a much larger signal than that from guanine groups alone and is much easier to be measured.

However, guanine bases are irreversibly oxidized in the first scan. As a result, $I_{\text{amplifiedG}}$ is only observed in the first scan while $I_{\text{mediators}}$ is always present and appears to be very stable. This makes it possible to derive the $I_{\text{amplifiedG}}$ by subtracting the data of the second scan from that of the first scan, i.e.

$$I_{\text{amplifiedG}} \approx I_1 - I_2 \propto [\text{G}]. \tag{2}$$

Hence, the difference between the first and second scans carries the quantitative information approximately proportional to the number of guanine groups presented at the electrode surface. Figure 4(b) shows the differential curve ($\Delta I_{1,2} = I_1 - I_2$) after subtracting the second scan from the first one, which gives a well-defined positive peak (red curve), i.e. $\Delta I_{p1,2} = I_{p1} - I_{p2} > 0$, where I_p is the peak current of a scan. The difference in peak current between the second and third scans, i.e. $(I_{p2} - I_{p3})$, is much smaller (as illustrated by the blue dotted curve). Further scans give almost flat or small negative peaks in the differential curves, i.e. $\Delta I_p \leqslant 0$. The small positive value in $(I_{p2} - I_{p3})$ indicates that there is still a very small amount of electroactive guanines left at the surface after the first scan, which is likely due to the fact that some guanine groups in the long single-stranded PCR amplicon dangles far

away from the electrode surface. On the other hand, the guanine groups in the much shorter oligonucleotide target that we used in the previous report [6] were completely oxidized after the first scan and gave a small negative peak in $(I_{p2} - I_{p3})$. Such small negative peaks between two consecutive scans is typically observed with a clean MWNT nanoelectrode array, i.e. a nanoelectrode array without any probe functionalized to the MWNTs. The clear difference in the polarity of $(I_{p1} - I_{p2})$ is attractive for disposable DNA chips in which subsequent scans directly serve as controls. Errors arising from the variation in using different electrodes for controls can be avoided with this approach.

The probe-functionalized electrodes incubated in the unrelated PCR amplicon with ∼400 bases also show negative values in $\Delta I_{p1,2}$. As shown in figure 4(c), the first scan gives a smaller ACV peak current, resulting in a negative peak in the differential curve, i.e. $\Delta I_{p1,2} = I_{p1} - I_{p2} < 0$ in figure 4(d). This confirms that the additional EC signal in the first scan, i.e. $I_{\text{amplifiedG}}$, can only be attributed to guanine bases from the specifically hybridized targets. The unmatched DNA molecules are completely removed from the electrode surface by stringent washing. The polarity of $(I_{p1} - I_{p2})$ can be directly used as the criteria for gene analysis. Further control measurements of the probe-functionalized MWNT nanoelectrode array after incubation in 10 μM 20 mer polyG solutions and the probe-functionalized electrode alone both give a consistent negative value of $(I_{p1} - I_{p2})$. The amplitude of $(I_{p1} - I_{p2})$ varies significantly from sample to sample due to the variation in MWNT density and size, which are not well-controlled without nanolithographic methods. However, this can be easily corrected by normalizing $(I_{p1} - I_{p2})$ with I_{p1}.

Figure 4(e) summarizes the mean value and the standard deviation of $(I_{p1} - I_{p2})/I_{p1}$ obtained from 21 experiments at five different conditions, with at least three experiments repeated at each condition. Clearly, the positive $(I_{p1} - I_{p2})/I_{p1}$ only appears upon the hybridization of the specific PCR amplicon. All four control experiments give negative values in $(I_{p1} - I_{p2})/I_{p1}$. Interestingly, the clean MWNT nanoelectrode array without any molecules bounded to the MWNTs gives the most reproducible results and a relatively small negative value in $(I_{p1} - I_{p2})/I_{p1}$. This is consistent with the fact that the first scan is always more sensitive to the adsorption of impurities and the state of the electrode surface. The presence of large nonelectroactive molecules such as the oligonucleotide probes at the electrode surface makes such phenomenon more evident in the other three control experiments. In subsequent scans, the electrode surface is cleaned up and activated, giving smaller and smaller ΔI_p. Normally, after three scans, all electrodes give small negative ΔI_p similar to the clean electrode.

4. Discussions and conclusions

With rigorous stringent washing, we have ensured nearly zero false positive. However, a certain percentage of false negative has been observed. Repeating nine experiments with the specific PCR amplicon, we obtained seven (78%) true positive and two (22%) false negative. Further studies are underway to coat the SiO_2 surface with organic thin films to reduce the nonspecific adsorption of biomolecules [21] so that a milder washing protocol can be employed, thus decreasing the false negative rate. In the mean time, we can use two electrodes for each test. The result is positive if either electrode measures a positive signal. In this way, the false negative can be reduced down to $22\% \times 22\% = \sim 5\%$. It needs to be noted that, while many nanotechnology based biosensors have shown sensitivities down to single molecular events, the signal may show a large fluctuation strongly depending on sampling and counting from the statistics point of view. Using an array of such nanoelements may provide better statistics and improve the reliability, which is critical for practical applications.

The number of signal moieties, i.e. guanine bases, in the PCR amplicon with ∼300 bases is statistically ∼75, which produces a large EC signal and allows us to use very low MWNT nanoelectrode densities. An array with an average MWNT diameter of 100 nm and nearest-neighbour distance of ∼2.5 μm grown on a $20 \times 20\ \mu\text{m}^2$ microcontact gives ∼70 MWNTs. From the previous discussion, there are no more than ∼70 PCR amplified targets hybridized on each MWNT, which gives a maximum of $\sim 70 \times 70 = 4900$ targets on each microcontact. In practice, this number could be much smaller than 1000 due to smaller MWNT diameter and lower hybridization efficiency. Such sensitivity is comparable to fluorescence-based DNA microarray techniques (with a limit of at least ∼300 hybridized targets per spot) [8]. Such ultrahigh sensitivity makes it possible for direct *in vitro* mRNA detection. In addition, the electronic platform makes the operation much simpler. By integrating with microfluidics, fully automated handheld devices can be developed for applications that require quick DNA/RNA analysis.

In summary, we have demonstrated that specific PCR amplicons can be directly and reliably measured using MWNT nanoelectrode arrays. This method is label-free since the inherent guanine bases in the DNA target serve as the signal moieties. The ultrahigh sensitivity, simple sample preparation, and easy operation of this electronic method are very attractive in developing low-cost handheld devices for early cancer diagnosis, pathogen detection and space exploration. The multiplex electronic DNA chip can be fabricated using conventional microfabrication techniques. A set of probes representing single nucleotide polymorphism, deletion and insertion in the BRCA1 gene have been designed and tested using a fluorescence-based DNA microarray [11]. Applying this multiplex assay onto the MWNT nanoelectrode array platform is underway, targeting the development of mass-produced disposable DNA chips for early cancer diagnostics.

Acknowledgments

Work by ELORET authors was supported by a NASA contract. We are grateful for helpful discussions with Professor James L Zehnder (Stanford Medical School) and financial support from the National Cancer Institute, under a contract with the Unconventional Innovations Program.

References

[1] Kuhr W G 2000 *Nat. Biotechnol.* **18** 1042
[2] Sosnowski R G, Tu E, Butler W F, O'Connell J P and Heller M J 1997 *Proc. Natl Acad. Sci. USA* **94** 1119

[3] Umek R M, Lin S W, Vielmetter J, Terbrueggen R H, Irvine B, Yu C J, Kayyem J F, Yowanto H, Blackburn G F, Farkas D H and Chen Y P 2001 *J. Mol. Diagn.* **3** 74
[4] Boon E M, Ceres D M, Drummond T G, Hill M G and Barton J K 2000 *Nat. Biotechnol.* **18** 1096
[5] Popovich N D and Thorp H H 2002 *Interface* **11** 30
[6] Li J, Ng H T, Cassell A, Fan W, Chen H, Ye Q, Koehne J, Han J and Meyyappan M 2003 *Nano Lett.* **3** 597
[7] Sistare M F, Holmberg R C and Thorp H H 1999 *J. Phys. Chem.* B **103** 10718
[8] Duggan D J, Bittner M, Chen Y, Meltzer P and Trent J M 1999 *Natl Genet. Suppl.* **21** 10
[9] Li J, Stevens R, Delzeit L, Ng H T, Cassell A, Han J and Meyyappan M 2002 *Appl. Phys. Lett.* **81** 910
[10] Li J, Ye Q, Cassell A, Ng H T, Stevens R, Han J and Meyyappan M 2003 *Appl. Phys. Lett.* **82** 2491
[11] Chen H, Han J, Li J and Meyyappan M 2003 *Genetic Testing* submitted
[12] McCreery R L 1991 *Electroanalytical Chemistry* vol 17, ed A J Bard (New York: Dekker) pp 221–374
[13] Miki Y, Swensen J, Shattuck-Eidens D, Futreal P A, Harshman K, Tavtigian S, Liu Q, Cochran C, Bennett L M and Ding W 1994 *Science* **266** 66
[14] Tinland B, Pluen A, Sturm J and Weill G 1997 *Macromolecules* **30** 5763
[15] Armistead P M and Thorp H H 2000 *Anal. Chem.* **72** 3764
[16] Wightman R M and Wipf D O 1989 *Electroanalytical Chemistry* vol 15, ed A J Bard (New York: Dekker) pp 267–353
[17] Wightman R M 1981 *Anal. Chem.* **53** 1125A
[18] Penner R M, Heben M J, Longin T L and Lewis N S 1990 *Science* **250** 1118
[19] Fan F R and Bard A 1995 *J. Sci.* **267** 871
[20] Menon V P and Martin C R 1995 *Anal. Chem.* **67** 1920
[21] Ostuni E, Chapman R G, Holmlin R E, Takayama S and Whitesides G M 2001 *Langmuir* **17** 5605